Dynamic Simulation of the THAI Heavy Oil Recovery Process

Muhammad Rabiu Ado[a], Malcolm Greaves[b], and Sean P. Rigby[a,*]

[a]*Department of Chemical and Environmental Engineering, University of Nottingham, University Park, Nottingham, NG7 2RD, U.K.*

[b] *Department of Chemical Engineering, University of Bath, Claverton Down, Bath, BA2 7AY U.K.*

* Corresponding author:

Tel: +44 (0) 115 951 4081, Email: enzspr@exmail.nottingham.ac.uk

Abstract

Toe-to-Heel Air Injection (THAI) is a variant of conventional In-Situ Combustion (ISC) that uses a horizontal production well to recover mobilised partially upgraded heavy oil. It has a number of advantages over other heavy oil recovery techniques such as high recovery potential. However, existing models are unable to predict the effect of the most important operational parameters, such as fuel availability and produced oxygen concentration, which will give rise to unsafe designs. Therefore, we have developed a new model that accurately predicts dynamic conditions in the reservoir and also is easily scalable to investigate different field scenarios. The model used a three component direct conversion cracking kinetics scheme, which does not depend on the stoichiometry of the products and, thus, reduces the extent of uncertainty in the simulation results as the number of unknowns is reduced. The oil production rate and cumulative oil produced were well predicted, with the latter deviating from the experimental value by only 4%. The improved ability of the model to emulate real process dynamics meant it also accurately predicted when the oxygen was first produced, thereby enabling a more accurate assessment to be made of when it would be safe to shut-in the process, prior to oxygen breakthrough occurring. The increasing trend in produced oxygen concentration following a step change in the injected oxygen rate by 33 % was closely replicated by the model. The new simulations have now elucidated the mechanism of oxygen production during the later stages of the experiment. The model has allowed limits to be placed on the air injection rates that ensure stability of operation. Unlike previous models, the new simulations have provided better quantitative prediction of fuel laydown, which is a key phenomenon that determines whether, or not, successful operation of the THAI process can be achieved. The new model has also shown that, for completely stable operation,

the combustion zone must be restricted to the upper portion of the sand pack, which can be achieved by using higher producer back pressure.

Keywords: bitumen; in-situ-combustion; oil recovery; simulation; kinetics

Introduction

According to the International Energy Agency[1] fossil fuels will continue to provide a dominant share of the world energy demand. While unconventional heavy oil/bitumen is predicted to account for an increasing share, against this back-drop, the contribution from conventional light oil is predicted to drop from 80% to 53% in the next two decades[2]. To-date, the vast reserves of the unconventional heavy oil/bitumen are virtually unexploited, even though current production totals are more than 2.5 million bopd (barrels of oil per day). Therefore, in a scenario where various economic and political constraints are likely to restrict energy supplies from both conventional hydrocarbons as well as from renewables, it is important to facilitate the use of advanced technologies to recover and upgrade the known heavy oil and bitumen resources, consistent with what is both economically and environmentally acceptable. One such technology that has been field tested with very encouraging results from two pilot field tests, though with limited commercial success, is Toe-to-Heel Air Injection (THAI). A fuller understanding of its merits and limitations requires the application of a more sophisticated reservoir simulation model that can accurately predict both dynamic and steady state conditions created in the reservoir.

The increasingly stringent restrictions on greenhouse gas emissions necessitates that heavy oil recovery processes must be able to limit harmful emissions. The THAI thermal heavy oil recovery process has unique potential to achieve this. The following are some of the attributes of THAI that should be realisable in the field:

- generates its own fuel in the reservoir to fully sustain the process
- does not require any natural gas or water, during normal operation
- can be made essentially self-sustaining, so that no net energy input is required
- carbon capture ready, for EOR or sequestration
- high oil recovery potential
- creates an underground ‘reactor’ for in-situ upgrading
- potential for one-step ‘heavy to light oil’ upgrading in-situ
- improved economics for heavy oil recovery
- in-situ reduction of sulphur, nitrogen and heavy metals
- It has a small surface-footprint

The study of in-situ combustion has been mostly carried out at the laboratory scale. This is usually performed with either a combustion tube[3-7] or 3D combustion cell[8-10]. Experiments help in understanding the process mechanisms and provide insight into what will happen in the reservoir. However, even at laboratory scale, the full physics of the processes taking place must be fully understood in order to develop a rigorous model that can be used for upscaling to field scenarios. In-

situ combustion (ISC) applied to heavy oil recovery is a very complex process. During conventional ISC, air is injected continuously through vertical injectors and the mobilized oil is produced via vertical production wells. An expanding combustion front is created by the continuous injection of air. This is sustained by continuous deposition of 'fuel' or coke due to thermal cracking of heavy residua ahead of the combustion front. The heat generated by the combustion reactions is transported towards the cold oil/bitumen by the generated steam and combustion gases and this causes a substantial viscosity reduction, allowing the oil to be displaced towards the production well.

Toe-to-Heel Air Injection (THAI) is a variant of the conventional ISC process, but uses a horizontal producer well instead of a vertical producer well. The combination of vertical injector(s) and a horizontal producer, i.e. VIHP and 2VIHP, arranged either in direct line-drive (DLD) or staggered-line drive (SLD), enables the mobilized oil ahead of the combustion front to flow downwards to the horizontal producer under gravity. Thus THAI is a gravity-stabilised process. Experiments[8-11], and also field scale developments[12], have consistently demonstrated robust and stable combustion front propagation. Turta and Singhal[13], Xia *et al.*[11], and Greaves *et al.*[14] have highlighted the advantages of THAI as a heavy oil recovery technique over conventional ISC and Steam Assisted Gravity Drainage (SAGD). Xia *et al.*[11] reported on the need to study ISC processes, both experimentally and numerically, in a 3-D arrangement in order to more fully understand the full physics of the process. However, despite the tremendous progress made through experimental studies, only a few models have been validated against 3D combustion cell experiments. To the best of our knowledge, only one such model exists in the literature.

Greaves *et al.*[15] developed a 3D combustion cell model using Computer Modelling Group's (CMG) STARS thermal simulator. The model, which was validated against a 3D combustion cell experiment using virgin Athabasca Oil Sands[8], predicted some of the dynamic features of THAI. However, it was not able to accurately predict certain critical parameters, such as fuel availability (fuel deposition) and also the effect of a sudden change in air injection rate on the level of produced oxygen. Although the steady-state trend of produced oxygen was predicted satisfactorily, there was a very large time delay in the response, which was probably due to the high fuel concentration predicted ahead of the combustion front. The combustion peak temperature was also over predicted by up to 90 ^{o}C for most of the dry combustion period. The model used a split-cracking kinetics scheme, as opposed to the direct conversion cracking kinetics scheme reported by Phillips *et al.*[16]. The major disadvantage of split-cracking kinetics is it is heavily dependent on the selected stoichiometric coefficients of the products. In addition, the viscosity used in the model is not typical of Athabasca bitumen[17]. Instead, the lower viscosity of Wolf Lake heavy oil, a default value in the STARS simulator, was used. Despite the use of the lower viscosity in their model, the fuel availability was still significantly over-predicted.

The main mechanism through which *fuel deposition* takes place during ISC remains a contentious issue. Fuel is considered to be deposited mainly by thermal cracking of the heavier fractions ahead of the combustion front[3,16]. However, authors such as Belgrave *et al.*[18], and Yang and Gates[6], reported that fuel deposition is mainly due to low temperature oxidation (LTO) taking place ahead of the combustion front. Alexander *et al.*[19], on the other hand, reported that LTO is only significant during the start-up period, when oil is present around the pre-heated zone and comes directly in contact with injected air. During 3D combustion cell experiments on Athabasca Oil Sands, the combustion zone temperature was consistently observed to be greater than 450 ^{o}C[8] and generally around 600 ^{o}C. Therefore, THAI mainly operates in a high temperature oxidation (HTO) mode, i.e. a vigorous high temperature state. This is absolutely essential for the heavy oil recovery process, to ensure that a stable combustion front propagates through the reservoir oil layer, with only a small, or nil, percentage of oxygen ahead of the combustion front, Accordingly, Greaves *et al.*[15] modelled their 3D combustion cell experiment excluding LTO reactions. Some authors[20,21] used kinetics validated against combustion tube experiments, but this type of experiment does not capture the full 3D nature of the processes taking place during ISC[11]. We investigated the effect of LTO reactions on fuel deposition. However, we only present the results of the model without LTO.

Numerical Modelling of THAI is a very challenging reservoir problem. This is due to the strongly coupled interaction between reaction kinetics and fluid flow processes in the reservoir. The kinetics of fuel (coke) deposition and coke combustion remain one of the major sources of uncertainty in modelling THAI, and also conventional in situ combustion. The complex nature of heavy crude oils also makes it impractical to use kinetics based on the actual number of components and therefore a smaller number of pseudo-components are usually employed. The deficiencies associated with current THAI numerical simulation models, have motivated us to develop a new model based on Phillips *et al.*[16] direct conversion cracking kinetics scheme. It is found that this kinetics scheme results in a significant decrease in the uncertainty in the simulation results, as it does not depend on the stoichiometry of the products. The improved accuracy and reliability of the new model also means that it can easily be scaled up to investigate the performance of THAI in different reservoirs.

Before attempting to scale-up a model for the THAI process to field-scale, which then necessitates the incorporation of additional levels of model complexity that will hinder fault detection and correction, it is important to ensure that the basic model is fully predictive of the general features of the process observable even at laboratory scale. It is critical to know the sensitivity of the model to its component parts, such as reaction kinetics, in order to be able to anticipate any impact from the likely variability at field-scale due to expected natural reservoir heterogeneities, given it is difficult to make measurements of such effects at field-scale. The sensitivity of the simulation to the reaction kinetics model will be tested by comparing the impact of the different kinetic schemes used here and in previous work[15]. It is also necessary to identify idiosyncratic features of the experimental-scale

behaviour, that need to be excluded in scale-up. The previous model available for THAI gave rise to predictions of the key observables of oil production rate and fuel lay-down where greater accuracy is needed for scale-up. Further, the experimental observations of produced oxygen were contradictory to the past model. It is, thus, the objective of this work to understand the causes of these aforementioned discrepancies, and, hence, develop a model that is robust and overcomes the drawbacks of the previous model, to provide a firmer basis for subsequent scale-up.

Methodology

Simulations were performed on a server with 2×ISRCPU-256-Intel Xeon 8 Core Processor E5-2680 20M Cache, 2.70 GHz. The findings from a 3D THAI experiment, using natural, virgin Athabasca bitumen, as reported by Xia and Greaves[8], has been used to validate the model developed in this work. CMG's STARS thermal reservoir simulator was used to develop a numerical model of the process. STARS incorporates a discretised wellbore (DW) option, which models the transient multiphase flow and heat transport in the horizontal producer (HP). The resulting equations are then coupled with the reservoir reaction and transport equations for simultaneous solution. Only the dry combustion period of the experiment is considered in the present study. After packing the combustion cell with virgin Athabasca Oil Sand, an electrical heater was used to pre-heat the zone around the horizontal injection (HI) well, referred to as Injector 1 (Fig.1). Air was then injected at a rate of 8000 $Scm^3\,min^{-1}$ which is equivalent to an air flux of 12 $m^3\,m^{-2}h^{-1}$. After 190 minutes, the air injection rate was increased by one-third, increasing the air injection flux to 16 $m^3m^{-2}h^{-1}$. This flux was maintained up to the end of the dry combustion period of 320 minutes.

Phillips *et al.*[16] kinetics parameters, obtained from their experiments on the thermal cracking of Athabasca bitumen, have been slightly adjusted for use in our model, as explained in the next section. However, the PVT data for the individual pseudo-components was generated separately, since this was not reported by Philips *et al.*[16].

PVT data: the Peng-Robinson Equation of State (PR-EOS) available in Aspen HYSYS software, was used to model the Athabasca bitumen using three pseudo-components (Tab. 1) based on the initial boiling point (IBP) data provided by Phillips *et al.*[16]. The pseudo-components and PVT data is given in Tab. 1, where LC, MC, and IC are defined as the light, mobile, and immobile pseudo-components respectively.

The variation of Athabasca bitumen viscosity with temperature was taken from Mojarab *et al.*[22] and the viscosities of the LC and MC fractions is similar to that of the ''Light oil'' and ''Heavy oil'' pseudo-components available in STARS. A linear mixing rule was used to estimate the viscosity of

the IC pseudo-component. Also, the phase equilibrium K-values were estimated based on Wilson's equation[23].

THAI kinetics: Table. 2 shows the original Phillips *et al.*[16] kinetics parameters and those used in the current study. The frequency factors and activation energies for Reactions 3 and 4 were 'tuned' using a trial and error search, in order to match the experimental parameters reported by Xia and Greaves[8]. They are, in-fact, still quite similar to the original Phillips *et al.*[16] values as the rate constant of the coke forming reaction at 400^{o}C is 97.5% of the original value. LC as defined in our model is initially present as a higher fraction (16 wt%) compared to the 10.3 wt% given by Phillips *et al.*[16].

The frequency factor for the coke combustion reaction and the heat of reaction were adjusted to best match the peak combustion temperature in the experiment. A constant $CO_2/(CO_2 + CO)$ ratio of 95 to 97 % was used to calculate the stoichiometry of the combustion reactions in order to match the experimental mole fractions. Each combustion reaction satisfies the respective mass balances, and the rounded stoichiometric coefficients are shown in Tab. 3. Although the combustion reactions for each pseudo-component are included in the model, their effect on the simulation results have been found to be insignificant. This is to be expected since, following ignition, the pre-heated inlet zone of the sandpack contains only residual coke – the other lighter fractions having been evaporated off. The establishment of an expanding vigorous combustion zone then also ensures that this process continues, leaving only coke as fuel for combustion.

Petrophysical parameters: The porosity and absolute permeability used (Tab. 4) were taken from Greaves *et al.*[15]. The adjusted oil/water relative permeability curve, shown in Fig. 2a, is based on data in Prowse *et al.*[17]. The gas/oil relative permeability curve has been adjusted to increase numerical stability consistent with the experimental results (Fig. 2b).

Grid Sensitivity: in order to choose the optimum mesh size, simulations were run for six different grid types (Tab. 5) in order to determine which one gave sufficient resolution to model the dynamics of the combustion zone, commensurate with computational efficiency (note run times in Tab. 5). The equations were solved using PARASOL which is a parallel processing solver available in STARS. We used 16 cores (i.e. 32 threads) computer to run the models. However, only 25% of the CPU is used as the maximum number of threads that can be specified to PARASOL is 8.

The effect of grid size on combustion peak temperature is not very significant, overall. As can be seen from Fig.3a, during the lower air flux period (up to 190 minutes), there is a divergence from the experimental trend after the initial start-up, but the difference subsequently diminishes considerably, after about 120 minutes, and even more so into the higher air flux period. As already mentioned, the earlier Greaves *et al.*[15] model was seriously deficient in that it failed to accurately predict the time

when oxygen was first detected at the production well. The previous model[15] predicted the oxygen would be produced after 280 min, compared to 170-180 mins in the experiment (a discrepancy of ~57%). In contrast, the new model predicted the production of oxygen at a time of 145-200 mins, depending on grid-size (Fig. 3b), which is a much reduced discrepancy of ~17%, even at worst. The 'fine dynamic mesh' was selected for the rest of the simulation study because it most accurately predicts this event (Fig. 3b), as well as the subsequent increasing trend, albeit in an oscillatory manner. The oscillations remained when the grid size was changed, and, thus, are unlikely to be due to artefacts in the solution. Further, it is noted that there is some indication (in Fig. 3b) of undulation in the experimental data itself, with local maxima in oxygen concentration at ~200, ~230, and ~310 mins, albeit not always as large in amplitude as the simulation. Further, the sampling of oxygen concentration in the experiments was discrete and periodic, rather than continuous, and thus the data sampling rate may have been insufficient to capture the full extent of periodicity in the experimental system. Similarly, the sampling is less frequent while measuring the experimental oil rate. The experimental sampling rate was generally every 15 minutes[8]. The other parameters in Fig. 3 are quite well-matched, especially the cumulative oil production. The prediction of oil upgrading is more variable, but generally lies within ±2 API points, and all of the different mesh predictions more or less converge on the same solution.

Results and Discussion

Start-up and Oil Production: Liang *et al.*[10] reported that one of the most critical factors affecting the overall stability of THAI was the start-up procedure. A distinct feature of the present model is that it takes into account the fact that no oil is present inside the horizontal producer (HP) prior to the pre-ignition heating cycle (PIHC). During the first 18 minutes of the PIHC, no oil was produced, because the oil has to first become mobile before it can flow to the HP (Fig. 4a). The use of electrical heaters to pre-heat the inlet zone of the sandpack, including near the toe of the horizontal injector (HI), results in the formation of thermally cracked products (gaseous/light hydrocarbons) causing a build-up in pressure around the toe of the HP during the start-up period. As a result, during the next 12 minutes (i.e. from 18 to 30 minutes), the predicted oil production rate greatly overshoots the experimental rate (Fig. 4a). The experimental oil rate did not show a spike because of the averaging out due to low sampling rate during the experimental measurement of the oil flow rate.

As the pressure in the combustion cell settles to a steady value, the predicted oil rate quickly converges on the experimental trend. Overall, the simulation showed good agreement with the experimental trend, particularly during the lower air flux period, where the deviation is less than 0.5 $cm^3\ min^{-1}$. There is also generally excellent agreement between the predicted and experimental trend

in cumulative oil production (Fig. 4b). At the end of the combustion period (Fig. 4b), the overall relative error is only 4%, compared to 7.2% in the results of Greaves *et al.*[15].

Peak Temperature: Fig. 4c shows a comparison of the experimental and the predicted peak combustion temperature variation with time. It can be seen that the observed temperature variation is complex in form, and, thus, is difficult to fit. However, Fig. 4c shows that a good overall agreement could be achieved over the whole time interval by fitting the Arrhenius parameters for the coking reaction for the kinetic model used here. In particular, there is a very good match of the maximum temperature following ignition (~900 ^{o}C) and also in the higher air flux period, after 190 minutes, which is better than was possible with the previous model[15]. However, there are some significant deviations during the first, lower air flux period. Here, the predicted peak combustion temperature twice undershoots by 100 ^{o}C, and also overshoots by a similar margin. It is possible that the tape heater control strategy employed in the experiment over-compensated for the heat loss, allowing the sandpack temperature to increase, and then under-compensated causing the temperature to undershoot. However the simulation prediction during the higher air flux period is excellent.

Oil Upgrading: There were some differences between the API gravity predicted by the model and what was observed experimentally (Fig. 4d), of up to ±4 ^{o}API between times of 20 and 120 minutes. These differences occur mainly during the first period, when the air injection flux was lower, being only 12 $m^3m^{-2}h^{-1}$. The trends tend to reflect the variations in the combustion peak temperature described previously. This is to be expected, since in-situ upgrading of the oil is mainly due to thermal cracking, the extent of which depends upon the temperatures generated in the combustion zone. There is, generally, a fairly good agreement between the experimental and simulated API gravity values, especially during the higher air flux period where the maximum deviation is 2 ^{o}API between 200 and 230 minutes. One slightly curious result is that, although the combustion peak temperature is slightly higher when the air flux is higher, the degree of oil upgrading is slightly lower on average, by about 1^{o}API.

Produced Oxygen: In the 3D combustion cell experiment[8], the gas composition showed that oxygen was first produced before the increase in air injection flux. This finding contradicted the assertion by Greaves *et al.*[15] that the first appearance of oxygen was due to the sudden increase in air injection rate. This therefore, warranted further investigation and was key to understanding the dynamic behaviour of THAI.

There are actually two possibilities as to why the produced oxygen began to increase before there was any increase in air injection rate. It could be due to a partial instability, in which case the oxygen response should either reach a new steady state or become zero. It could also have been due to channelling of air between the combustion cell wall and the sand pack, but this is not very likely because the experimental oxygen response appears to tend to a steady state after 310 minute (Fig. 5a).

Further, Xia and Greaves[8] did not report any problem of this sort during the experiment. However, because the dry combustion experiment lasted for only another 10 minutes (to 320 minutes), it is impossible to conclude this with any certainty. It can be seen from Fig 3b and Fig. 5a that the start of the oxygen increase in the producer well is much more accurately predicted than by the previous model[15], irrespective of grid size used, and the subsequent increasing trend is also well predicted, up to the end of the dry combustion period.

In order to investigate if there was any other potential reason for oxygen increasing in the producer well, the simulation was run again, but this time with the air flux maintained at 12 $m^3m^{-2}h^{-1}$ for the whole dry combustion period. The increase in oxygen (Fig. 5b) occurred at exactly the same time, regardless of whether the injected air flux was increased or not. The overall trend was similar in both cases. The lower flux curve overlies the higher flux curve by a fraction of a percent. At the end of the dry combustion period, the fuel availability increased by up to 4 kgm^{-3} (33 %) due to the increase in air injection flux.

Shape of Combustion Front and Oxygen Utilisation: During the dry in situ combustion period, the region swept by the combustion front had 100% gas saturation[24]. The same should apply in THAI, so that the region behind the combustion front will be occupied by injected air. The shape, or leading edge of the combustion front should coincide with the boundary where the oxygen concentration falls to zero[15]. Fig. 6 provides an indication of the approximate shape of the combustion front, since the oxygen concentration at the leading edge of the combustion front is not everywhere zero.

The combustion zone in the upper part of the sandpack (Fig. 6a) has expanded across the entire width of the cell by 150 minutes after the start of air injection. There is a gradual tapering of the combusted zone, downwards towards the horizontal well, as the combustion front advances through the sandpack (Fig. 6b). After 320 minutes (Fig. 6b), the burned zone covers about 30 % of the sandpack.

Fig. 7a also shows that, in the vertical mid-plane, the combustion front is about 2 cm away from the toe of the HP. Since the combustion front velocity is steady at 6 cm h^{-1} over the next 20 minutes, the inlet region of the sandpack, up to the toe of the HP, will therefore have been swept by the combustion front. Most strikingly, in Fig. 7b, although there is oxygen in the HP along about 30 % of its length from the injection end of the sandpack, downstream of this there is no oxygen present. Nevertheless, increasing the air injection flux by 33 % would be expected to push the process much closer to instability, and in practice, therefore, it would be safer to design for a lower air injection rate. Even though the oxygen concentration in the HP reaches up to 10 % for about one-third the distance from the toe, it then decreases to almost zero.

Fuel Availability: In this study, a substantial improvement in predicting the fuel laydown has been achieved, compared to the result of Greaves *et al.*[15]. At the end of the dry combustion period at 320

minutes, the predicted average fuel availability is 52.3 kgm^{-3} of reservoir volume. Greaves *et al.*[15] predicted an average fuel concentration of 85.4 kgm^{-3}. The predicted fuel laydown ahead of the combustion front has, therefore, been reduced by over 40% giving a value which lies within the expected range for Athabasca Oil Sands. Based on the work of Alexander *et al.* [19], the estimate for fuel availability for Athabasca bitumen, with H/C = 1.53 and API gravity of 9 points, at 25 ^{o}C, ranges from 50 to 57 kgm^{-3} of bulk reservoir volume.

It is clear from Fig. 8 that the predicted fuel concentration varies considerably, depending on position in the sandpack. The fuel concentration immediately ahead of the combustion front remains constant, in the range of 35 to 40 kgm^{-3}. Traversing downwards through the sandpack there is an increase in the fuel concentration from 40 to 139 kgm^{-3}. The highest coke concentration is found in the bottom layer of the sandpack, directly below the HP. Because the mobilized oil flows by gravity towards the HP, generally less coke is deposited along the vertical mid-plane. This is because this is the region which experiences the most intense drawdown. The form of the coke profiles in Fig. 8 are very similar to those obtained from the post-mortem examination of the 3D THAI combustion cell experiment[15]. The region swept by the expanding combustion front has zero coke concentration, which is a finding that has also been reported by Chen *et al.*[25] after conducting their post-mortem analysis.

Temperature Distributions: the simulated temperature distributions (Fig. 9) provide a more detailed indication of the extent of the combustion reaction and heat transfer in the sandpack, not easily obtained from experimental measurements. The different regions over which LTO (low temperature oxidation) and HTO (high temperature oxidation) take place are usually identified by specific ranges of temperature. The top horizontal plane and vertical mid-plane temperature profiles are presented in Fig. 9. The temperature around the combustion zone is generally greater than 400 ^{o}C, implying that only coke combustion takes place there, and hence the incidence of LTO is negligible.

Oil Saturation: In Fig. 10, the Mobile Oil Zone (MOZ) is identified by the oil flux vectors superimposed on the oil saturation profile. They indicate the relative magnitudes of oil flow rate. The temperature in the MOZ (Fig. 9) along the horizontal well axis ranges from 100 ^{o}C near the cold oil layer, to around 250 ^{o}C upstream of this, at the trailing edge. Further out into the predominantly cold oil zone of the sandpack, the highest temperatures are about 50 ^{o}C lower than this. It is also very evident that oil banking occurs immediately ahead of the MOZ. The distance between the trailing edge of the MOZ and the combustion front is the main determinant affecting the temperature of the MOZ, and hence, the rate at which oil drains into the horizontal well. Overall, the distance varies from about 5 to 8 cm in Fig. 10, over the 170 minutes of combustion time. This is equivalent to 7 to 15 % of the length of the sandpack (or horizontal producer well). In the field, this would be equivalent to approximately 35 to 70 metres for a 500 m long HP. For the most part, the oil rate vectors are either vertical or forward leaning, downwards, into the HP. There are also upwards-directed vectors,

indicating that there is significant flow of oil from beneath and into the HP. The smaller oil rate vectors located in the cold oil zone, indicate that some oil drainage occur there. Overall then, the picture is one of higher oil rate from the upstream section of the MOZ from a region of lower oil saturation (25 to 60 %), but lower rates (about half) from the banked oil region ahead of it, where the oil saturation is highest (80 to 100%), but also colder.

Conclusions

The new model underlying the more accurate simulations of THAI presented here improves our understanding of the internal mechanism of the complex coupled reaction-transport system underlying successful operation of the process. Several particular advances in understanding have been made due to particular changes made to previous models, and these are summarised below.

The Phillips *et al.*[16] thermal cracking kinetics scheme, together with PVT data estimated using the PR-EOS, have been used to develop a more accurate numerical simulation of the Xia and Greaves[8] 3D THAI combustion cell experiment than achieved previously; this was for the dry combustion part of the experiment. The new model used three oil pseudo-components, as opposed to the two used by the previous model of Greaves *et al.*[15]. The new THAI model is also more accurately scale-able for field studies than the previous model, since the stoichiometry of the fuel formation reaction is directly fixed by the relative molecular mass of the pseudo-component.

The simulation presented here provided a better match than the previous model[15] for the oil rate, cumulative oil production, peak combustion temperature, and produced oxygen concentration over the dry combustion period of the experiment. However, the API gravity of the upgraded produced oil is over-predicted by up to 2 API points, although during certain periods of the experiment there is much closer agreement.

The simulation presented here provided new insight, not available previously[15], into the mechanism of oxygen production during the later stages of the experiment. Oxygen is first produced towards the end of the low air injection rate period. The increasing trend of produced oxygen was predicted following a step change in the injected oxygen rate of 33 %. The temperatures profiles in the sandpack indicate that safe operation of the THAI process can be maintained using an air injection rate slightly lower than the lowest air rate used in the experiment.

The new model provides a more accurate prediction of the fuel availability, averaged over the sandpack volume, than possible before[15]. The predicted range is in agreement with typical values reported for Athabasca Oil Sands bitumen.

The new simulation also provides better guidance on the operability of the process than available before. The shape of the combustion front before any oxygen is produced is forward leaning, indicating that the process is entirely stable. Once the combustion front reaches the toe of the horizontal producer well, it tends to become more vertical and this is an indication that the process is marginally stable. This means that any further increase in the air injection rate will cause instability. The simulation also shows that for completely stable combustion front propagation, the combustion zone should be restricted to the upper part of the sandpack. Otherwise, coke must be present inside the horizontal production well in order to prevent oxygen being produced.

References

1. IEA. *Key World Energy Statistics*. 2013 [cited 2013 22 Dec]; Available from: http://www.iea.org/.
2. IEA. *World Energy Outlook 2013 Factsheet*. 2013 [cited 2013 22 Dec]; Available from: http://www.worldenergyoutlook.org/.
3. Lin, C. *Old SPE Journal*, **1984**, *24*, 657-666.
4. Bagci, S.; Kok, M.V. *Energy & Fuels*, **2004**., *18*, 1472-1481.
5. Razzaghi, S., et al., *J. Japan Pet. Inst*., **2008**, *51*, 287-297287.
6. Yang, X.; Gates, I. *Natural Resources Res.*, **2009**, *18*, 193-211.
7. Kovscek, A.; Castanier, L.; Gerritsen, M. *SPE Reserv. Eval. & Eng.* **2013**, *16*, 172-182.
8. Xia, T. ; Greaves, M. *J. Can. Pet. Technol*., **2002**, *41*, 51-57.
9. Xia, T., *THAI Process-Effect of Oil Layer Thickness on Heavy Oil Recovery*. in *Canadian International Petroleum Conference*. 2002.
10. Liang, J., *Pet. Explor. & Dev*., **2012**, *39*, 764-772.
11. Xia, T.; Greaves, M.; Turta, A. *J. Can. Pet. Technol*., **2005**, *44*, 42-48.
12. Petrobank. *Petrobank Announces Q1 2014 Financial and Operating Results*. 2014 [cited 2014 20 May]; Available from: http://www.petrobank.com/news.
13. Turta, A. ; Singhal, A. *J. Can. Pet. Technol.*, **2004**, ***43***, 29-38.
14. Greaves, M.; Xia, T.; Turta, A. *J. Can. Pet. Technol.*, **2008**, *47*, 65-73.
15. Greaves, M., Dong, L.; Rigby, S.P. *Energy & Fuels*, **2012**, *26*, 1656-1669.
16. Phillips, C.R.; Haidar, N.I.; Poon, Y.C. *Fuel*, **1985**, *64*, 678-691.
17. Prowse, D.R., *Some Physical Properties of Bitumen and Oil Sand*, O.S.R. Department, Editor., Alberta Research Council: Edmonton, Alberta, 1983.
18. Belgrave, J., *A comprehensive approach to in-situ combustion modeling*. SPE Advanced Technology Series, 1993. **1**(1): p. 98-107.
19. Alexander, J.; Martin, W.L.; Dew, J. J. Pet. Technol., **1962**, *14*, 1154-1164.
20. Lim, G.; Coates, R.; Ivory, J. Gravity stable combustion processes for Athabasca oil sand reservoirs. in *World Heavy Oil Congress 2008*, Vol.2, Edmonton, Alberta, Canada, 10-12 March, 2008, 660-672.
21. Fatemi, S.; Ghotbi, C.; Kharrat, R. Brazilian J. Pet. & Gas, **2009**, *3*, 11-28
22. Mojarab, M.; Harding, T.; Maini, B. J. Can. Pet. Technol. **2011**, *50*, 9-18.
23. Almehaideb, R.; Ashour, I.; El-Fattah, K.. Fuel, **2003**, *82*, 1057-1065.
24. Burger, J.; Sourieau, P.; Combarnous, M. *Thermal methods of oil recovery*. Gulf Publishing Company, Book Division, 1985.
25. Chen, J.X., In Situ Combustion as a Followup Process to CHOPS. in *SPE Heavy Oil Conference Canada*, Society of Petroleum Engineers, 2012.

FIGURES

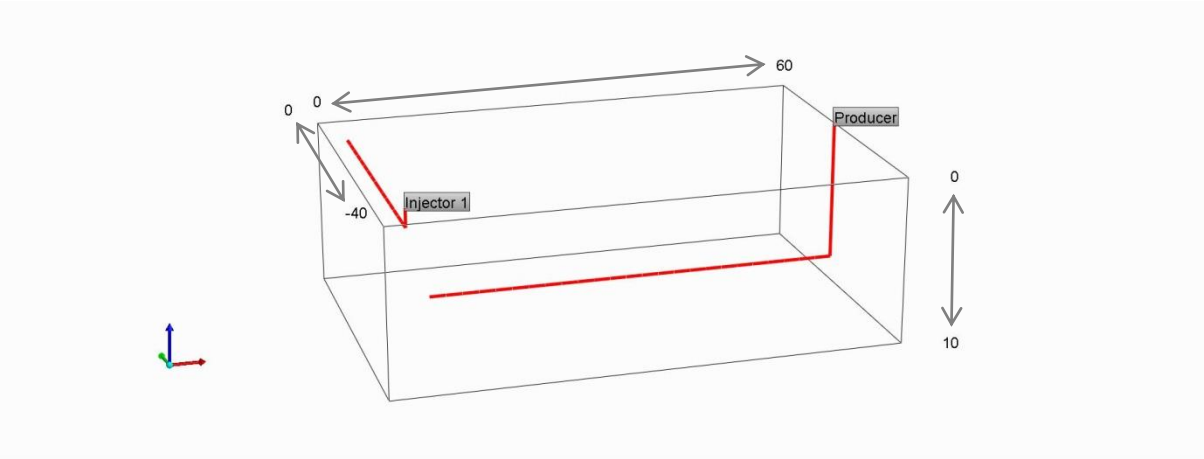

Figure 1: 3D Combustion Cell showing horizontal injector (HI) and horizontal producer (HP) arranged in direct-line drive. All dimensions are in cm [15]

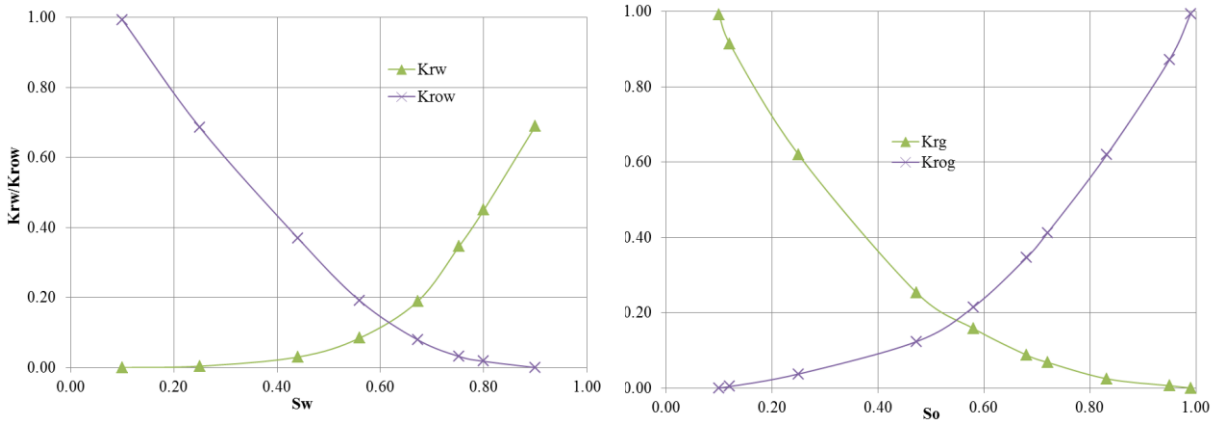

(a) (b)

Figure 2: (a) oil/water and (b) gas/oil relative permeability curves for Athabasca bitumen [17]. K_{rw} and K_{row} are the water and oil relative permeabilities at water saturation S_w respectively while K_{rg} and K_{rog} are the gas and oil relative permeabilities at oil saturation S_g respectively.

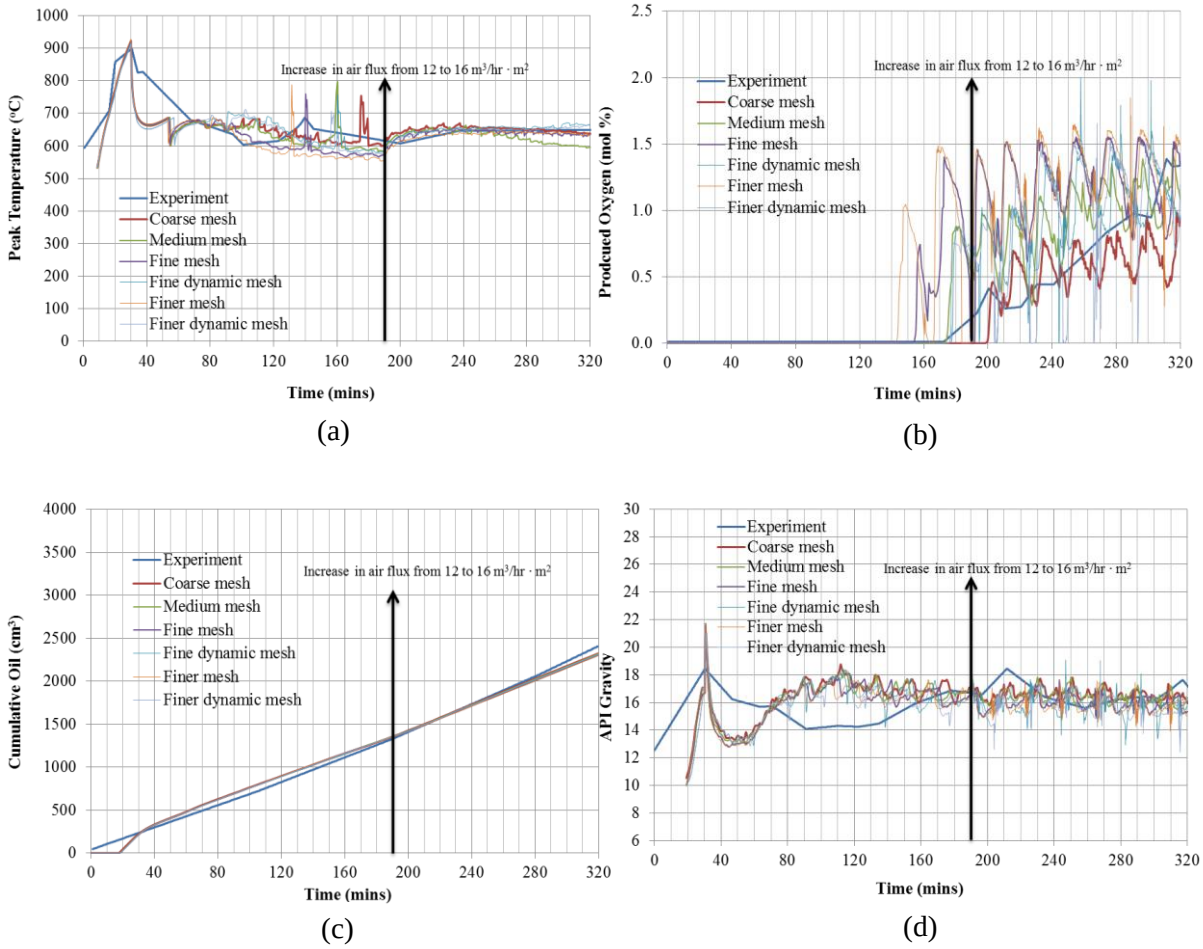

Figure 3: Effect of different grid sizes on (a) Peak combustion temperature, (b) Produced oxygen, (c) Cumulative oil production, and (d) Degree of upgrading

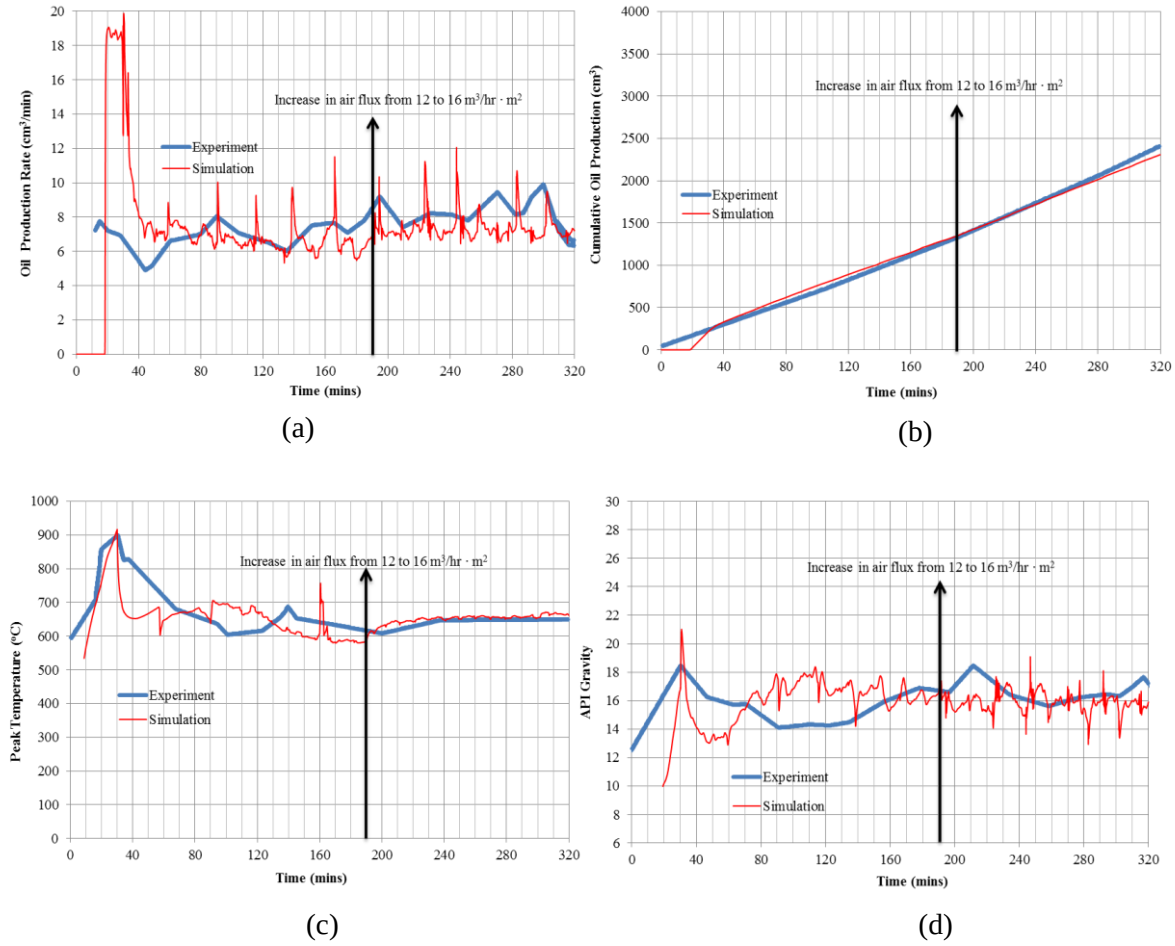

Figure 4: (a) Oil production rate, (b) Cumulative oil production, (c) Peak temperature, (d) API gravity

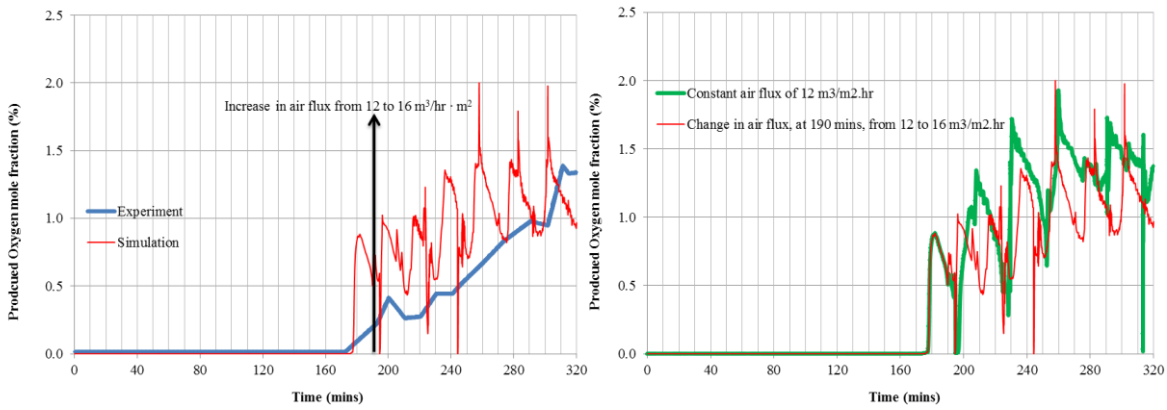

(a) (b)

Figure 5: (a) Experimental and simulated produced oxygen mole fraction, (b) Effect of increase in air flux on the produced oxygen concentration

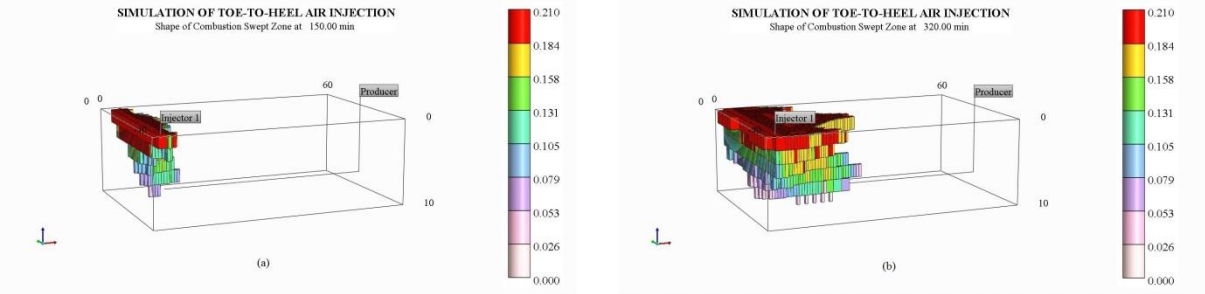

Figure 6: Oxygen mole fraction profiles indicating the approximate shape of the combustion zone after: (a) 150 minutes and (b) 320 minutes

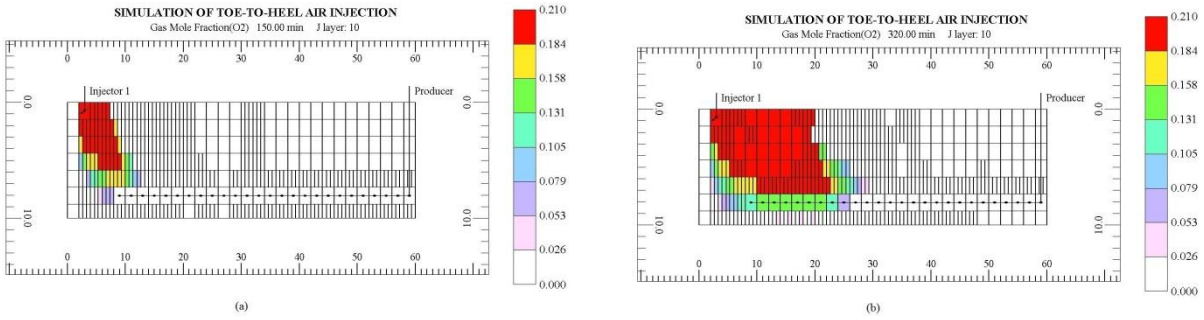

Figure 7: Oxygen mole fraction profiles along vertical mid-plane after (a) 150 minutes and (b) 320 minutes

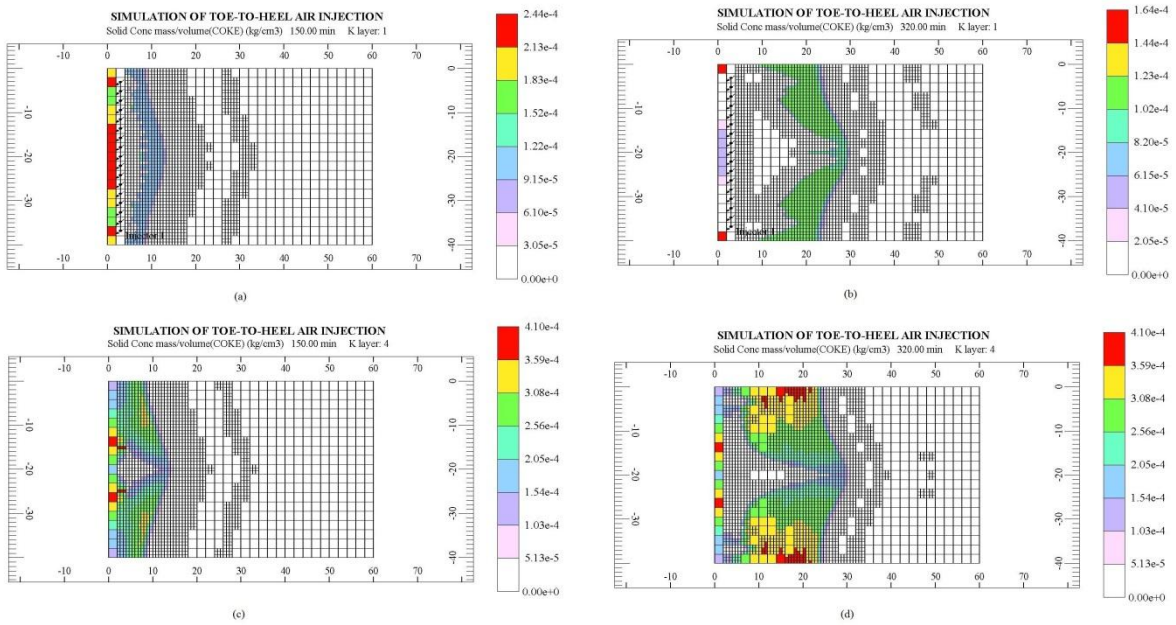

Figure 8: Coke concentration profiles (kgcm^{-3}); at top horizontal plane after (a) 150 minutes and (b) 320 minutes; at middle horizontal plane after (c) 150 minutes and (d) 320 minutes

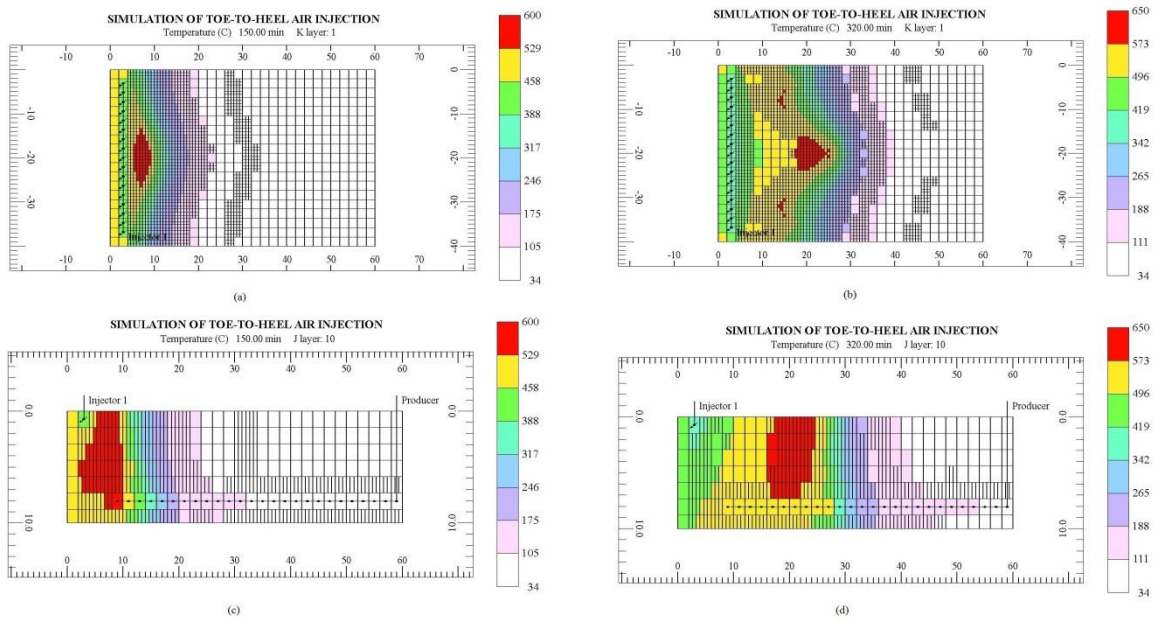

Figure 9: Temperature distribution: top horizontal plane after (a) 150 minutes and (b) 320 minutes; vertical mid-plane after (c) 150 minutes and (d) 320 minutes

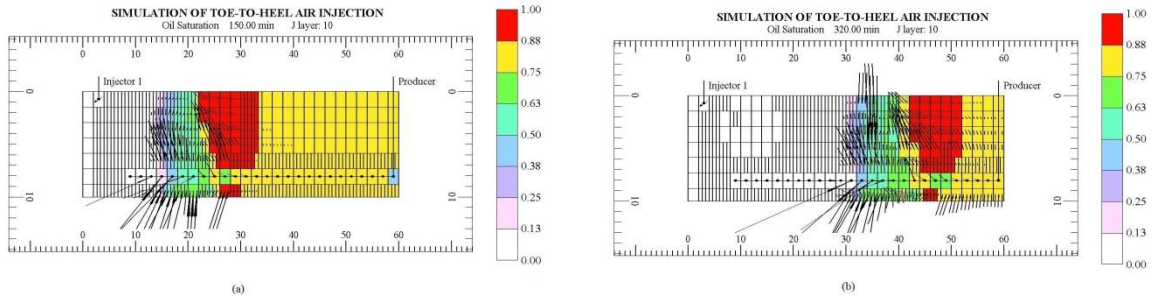

Figure 10: Oil saturation along vertical mid-plane after (a) 120 minutes and (b) 290 minutes of the start of ignition

TABLES

Table 1: PVT data used in the current study

Components	Fraction (mol%)	Molecular weight(g mol^{-1})	P_c (kPa)	T_c (^oC)	ρ (kg m^{-3})	Eccentricity	T_B (^oC)
LC	42.50	210.82	1682.88	464.68	828.24	0.62	281.47
MC	23.91	496.81	1038.46	698.53	961.66	1.18	549.67
IC	33.59	1017.01	729.22	940.36	1088.04	1.44	785.78

Table 2: Phillips *et al.* [16] and adjusted kinetics parameters for Athabasca bitumen-sand mixture

Reaction	Thermal Cracking Reactions	Phillips et al., (1985)		Current study	
		Frequency Factor (min^{-1})	Activation Energy (kJ/mol)	Freq. Factor (min^{-1})	Act. Energy (kJ/mol)
1	IC ➔ 2.0471 MC	3.822×10^{20}	239.01	3.822×10^{20}	239.01
2	MC ➔ 0.4885 IC	3.366×10^{18}	215.82	3.366×10^{18}	215.82
3	MC ➔ 2.3567 LC	3.132×10^{15}	180.88	1.132×10^{15}	184.88
4	LC ➔ 0.4243 MC	1.224×10^{15}	180.95	1.524×10^{15}	180.45
5	IC ➔ 77.4563 COKE	6.960×10^{14}	174.28	2.320×10^{15}	180.88

Table 3: Combustion reactions and respective kinetic parameters

Combustion Reactions	Frequency Factor (kPa min^{-1})	Activation Energy (kJ/mol)	Heat of Reaction (kJ/mol)
IC + 106.7 O_2 ➔ 78.9 CO_2 + 4.2 CO + 46.9 H_2O	1.812×10^8	138.00	4.00×10^4
MC + 37.1 O_2 ➔ 28.1 CO_2 + 1.5 CO + 22.4 H_2O	1.812×10^9	138.00	1.60×10^4
LC + 32.025 O_2 ➔ 11.2 CO_2 + 0.6 CO + 14.5 H_2O	1.812×10^{10}	138.00	4.91×10^2
COKE + 1.22 O_2 ➔ 0.93 CO_2 + 0.03 CO+ 0.57 H_2O	1.000×10^{10}	123.00	3.90×10^2

Table 4: Fluid saturation, porosity and absolute permeability [15]

S_o	S_w	Porosity	Vertical permeability (mD)	Horizontal permeability (mD)
0.85	0.15	0.34	3450	11500

Table 5: Number of grid blocks and time elapsed for numerical convergence

Grid	Number of blocks	Run Time (hr)	GBs sizes in $\boldsymbol{i} \times \boldsymbol{j} \times \boldsymbol{k}$ (cm $\times$cm $\times$cm)
Coarse Mesh	12,000	0.43	$1.000 \times 2.105 \times 1.467$
Medium Mesh	19,000	1.13	$1.000 \times 1.053 \times 1.467$
Fine Mesh	38,000	3.80	$0.667 \times 0.702 \times 1.467$
Fine Dynamic Mesh	38,000	2.40	$0.667 \times 0.702 \times 1.467$
Finer Mesh	50,000	5.48	$0.500 \times 0.702 \times 1.467$
Finer Dynamic Mesh	50,000	2.88	$0.500 \times 0.702 \times 1.467$

Note: The bottom horizontal plane, below the HP well, has the same thickness of grid-blocks of 1.2 cm regardless of the grid system.